



1 **The response of the regional longwave radiation balance and climate system**
2 **in Europe to an idealized afforestation experiment**

3
4 Marcus Breil^{1,2}, Felix Krawczyk², Joaquim G. Pinto²

5
6 ¹Institute of Physics and Meteorology, University of Hohenheim, Stuttgart, Germany

7 ²Institute for Meteorology and Climate Research, Karlsruhe Institute of Technology, Karlsruhe,
8 Germany

9
10 *Correspondence to:* Marcus Breil (marcus.breil@uni-hohenheim.de)

11
12
13
14
15
16
17
18
19
20
21
22
23
24
25
26
27
28
29
30
31
32
33
34
35



36 **Abstract**

37 Afforestation is an important mitigation strategy to climate change due to its carbon sequestration
38 potential. Besides this positive biogeochemical effect on global CO₂ concentrations, afforestation also
39 affects the regional climate by changing the biogeophysical land surface characteristics. In this study,
40 we investigate the effects of an idealized global CO₂ reduction to pre-industrial conditions by a Europe-
41 wide afforestation experiment on the regional longwave radiation balance, starting in the year 1986
42 from a continent entirely covered with grassland. Results show that the impact of biogeophysical
43 processes on the surface temperatures is much stronger than of biogeochemical processes.
44 Furthermore, biogeophysically induced changes of the surface temperatures, atmospheric
45 temperatures and moisture concentrations are as important for the regional greenhouse effect as the
46 global CO₂ reduction. While the greenhouse effect is strengthened in winter, it is weakened in summer.
47 On annual total, a Europe-wide afforestation has a regional warming effect, despite reduced CO₂
48 concentrations. Thus, even for an idealized reduction of the global CO₂ concentrations to pre-industrial
49 levels, the European climate response to afforestation would still be dominated by its biogeophysical
50 effects.

51

52 **1. Introduction**

53 A highly debated strategy to achieve the Paris climate targets is afforestation (Harper et al., 2018; Roe
54 et al., 2019). During their growth period, forests remove CO₂ from the atmosphere and store the
55 carbon in their biomass (Luyssaert, et al., 2010; Pan et al., 2011). CO₂ concentrations in the atmosphere
56 are consequently reduced, resulting in a reduction of the downwelling longwave radiation (DLR) and
57 an increase of the outgoing longwave radiation at the top of the atmosphere (OLR). In this way,
58 afforestation actively reduces the greenhouse effect itself.

59 Besides this positive biogeochemical impact on the global climate system, afforestation affects also
60 the regional climate by changing the biogeophysical characteristics of the land surface (Pielke et al.,
61 2011; Bright et al., 2017). In general, the albedo of forests is lower than of other natural land use forms.
62 As a result, more shortwave radiation is absorbed, counteracting the increased OLR (Bala et al, 2007;
63 Bonan, 2008). Thus, the regional climate benefit of afforestation depends on the weighting between
64 biogeochemical changes of the longwave radiation balance and biogeophysical changes of the
65 shortwave radiation balance (Claussen et al., 2001; Pielke et al., 2011).

66 Moreover, biogeophysical changes with afforestation have also a direct effect on the longwave
67 radiation balance. By changing land surface characteristics like albedo, surface roughness or leaf area
68 index, surface temperatures are altered (Lee et al., 2011; Duveiller et al., 2018). Since longwave
69 radiation emissions from the surface are, according to the Stefan-Boltzmann law, a function of the
70 surface temperature (T_s), changes in the longwave radiation emissions follow (Vargas Zeppetello et al.,



71 2019). Moreover, changes in the land surface characteristics with afforestation generally lead to an
72 increase of the turbulent heat fluxes (Burakowski et al., 2018; Breil et al., 2020). Atmospheric
73 temperatures (T_a) are consequently increased (Alkama & Cescatti, 2016; Breil et al., 2020), which in
74 turn affect the longwave radiation emitted by the atmosphere. Furthermore, changes in the
75 evapotranspiration rates alter the water vapor concentrations in the atmosphere (Q_a) (Bonan, 2008).
76 Since water vapor is known to be an important greenhouse gas, changes in its concentrations also
77 affect the atmospheric longwave radiation emissions (Claussen et al., 2001; Swann et al., 2010).
78 In spite of their relevance, these complex biogeophysically induced changes in the longwave radiation
79 balance are generally not considered in the ongoing debate on afforestation as a regional mitigation
80 strategy. The focus is often only on the biogeochemically induced CO_2 reduction and the
81 biogeophysically induced changes in the albedo (Claussen et al., 2001; Bala et al., 2007). An all-inclusive
82 understanding of the interrelation between afforestation and the greenhouse effect is thus missing.
83 The arising question whether biogeophysical changes are regionally strengthening or weakening the
84 positive biogeochemical impact of afforestation on the greenhouse effect is thus not yet answered.
85 The goal of this study is to disentangle the contribution of both biogeochemical and biogeophysical
86 processes on the emitted longwave radiation over Europe, in a step towards a physically based
87 comprehensive assessment of afforestation as a regional mitigation strategy to climate change.
88 The study is embedded in the Land Use and Climate Across Scales (LUCAS) project (Davin et al., 2020).
89 LUCAS aims to investigate the impact of land use changes on the European climate by performing
90 Regional Climate Model (RCM) simulations. In the first phase of the project, idealized afforestation
91 experiments were performed. In one experiment, the whole European continent was covered by forest
92 (FOREST), in the other experiment the whole continent was covered by grassland (GRASS). By means
93 of these idealized simulations, the maximum possible effect of afforestation on the European climate
94 could be estimated (Davin et al., 2020; Breil et al., 2020). However, only biogeophysical effects of
95 afforestation are considered in these simulations, since the carbon cycle is generally not included in
96 RCMs. Thus, the removal of CO_2 from the atmosphere was not taken into account.
97 In order to close this gap, an additional FOREST simulation which considers the reduced CO_2
98 concentrations with afforestation (CARBON) is analyzed. By comparing the results of CARBON, FOREST
99 and GRASS with the results of an offline radiative transfer model, the respective contributions of
100 biogeochemical and biogeophysical processes to the regional climate system, and particularly to the
101 longwave radiation balance, can be quantified. Section 2 describes the used methodology. The main
102 results are presented (section 3), followed by the discussion (section 4) and conclusions (section 5).

103

104 **2. Methods**

105 **2.1. RCM simulations**



106 All simulations (GRASS, FOREST, CARBON) are performed with the RCM CCLM-VEG3D (Breil et al., 2021)
107 for the Coordinated Downscaling Experiment – European Domain (EURO-CORDEX; Jacob et al., 2014)
108 on a horizontal resolution of 0.44° (~50 km). The simulations were driven by ERA-Interim reanalyses
109 (Dee et al., 2011) at the lateral boundaries and the lower boundary over sea. The simulation period is
110 1986–2015. A spin-up of 7 years was performed before 1986. The applied land use datasets are derived
111 from a MODIS-based present-day land cover map (Lawrence and Chase, 2007), in which the land use
112 classes in each grid cell were set to forest (FOREST, CARBON) or grassland (GRASS), respectively,
113 excluding deserts and glaciers (Davin et al., 2020). In CARBON, the resulting reduction in global CO₂
114 concentrations by an idealized Europe-wide afforestation (see section 2.2) is implemented in CCLM-
115 VEG3D, replacing the historic CO₂ concentrations used in FOREST and GRASS.

116

117 **2.2. Carbon sequestration by an idealized Europe-wide afforestation**

118 In this idealized afforestation experiment, the whole European continent is afforested, starting from a
119 continent entirely covered with grassland. Fig. 1 shows the respective partitioning of the afforested
120 area in boreal and temperate forests. In this experiment, 405 million hectares of Europe are covered
121 with boreal forests, 848 million hectares with temperate forests, thus 1.253 billion hectares in total.
122 On the basis of recent forest inventory data and the results of long-term ecosystem studies, Pan et al.
123 (2011) estimated the amount of carbon sequestered (biomass + soil) in boreal forests to 239 MgC per
124 hectare, and 155 MgC per hectare in temperate forests. This yields a total amount of 228.3 PgC
125 sequestered by a Europe-wide afforestation.

126 The arising global CO₂ concentrations from this idealized afforestation are calculated according to an
127 analytical approach of Goodwin et al. (2007). Assuming a mature forest and steady-state conditions
128 between the atmosphere and the buffering ocean-mixed-layer on a centennial timescale, changes in
129 the atmospheric CO₂ partial pressure P_{CO_2} are calculated as follows:

130

$$131 \quad \Delta P_{CO_2} = \int_{\Sigma C_1}^{\Sigma C_2} \frac{P_{CO_2}}{I_B} d\Sigma C \quad \text{Eq. (1),}$$

132

133 where I_B is the total carbon inventory of the atmosphere plus the total buffered carbon inventory of
134 the ocean. $d\Sigma C$ is the change in the total amount of carbon in the atmosphere-ocean system. Assuming
135 furthermore that changes in I_B are small compared to the total buffered inventory, Eq. (1) can be
136 integrated to

$$137 \quad P_{CO_2} = P_i e^{\frac{\Delta \Sigma C}{I_B}} \quad \text{Eq. (2),}$$

138 where P_i is the initial partial pressure of carbon dioxide at pre-industrial conditions. $\Delta \Sigma C$ is the
139 difference between the total anthropogenic carbon emissions until the year 1986 when our simulation



140 starts (based on Gütschow et al., 2019), and the amount of carbon that would have been removed
141 from the atmosphere by an idealized Europe-wide afforestation. Terrestrial emissions caused by land
142 use changes are not considered, since land emissions are balanced by the terrestrial CO₂ sink of
143 enhanced plant growth and the lengthening of the growing season (Friedlingstein et al., 2020).
144 According to Eq. (2), a resulting global CO₂ concentration of 279 ppm is calculated, constituting an
145 equilibrium on a centennial timescale. Thus, an idealized Europe-wide afforestation would have
146 reduced the global CO₂ concentrations at the beginning of our simulation period to pre-industrial
147 levels. This global CO₂ concentration is then implemented in the CARBON simulation.

148

149 **2.3. BUGSrad**

150 Longwave radiation (DLR and OLR) is an implicit function of T_s , T_a , Q_a and the CO₂ concentrations. While
151 the individual contribution of CO₂ on changes in DLR and OLR can be derived from the difference
152 between CARBON and FOREST, such an attribution is not possible for T_s , T_a and Q_a . Thus, DLR and OLR
153 are additionally recalculated with the offline radiative transfer model BUGSrad (Stephens et al., 2001).
154 BUGSrad solves the radiative transfer equation under the assumption of a plane-parallel atmosphere
155 as proposed by Ritter and Geleyn (1992). Thus, BUGSrad is using the same radiative transfer scheme
156 as it is implemented in CCLM-VEG3D, enabling a direct comparison with the RCM results. However,
157 the radiative schemes in CCLM-VEG3D and BUGSrad are not completely identical. BUGSrad is set up
158 with 6 shortwave and 12 longwave bands, whereas CCLM-VEG3D is set up with 3 shortwave and 5
159 longwave bands.

160 The calculations in BUGSrad are based on mean seasonal profiles of T , Q and pressure simulated in
161 CCLM-VEG3D. Only clear-sky situations (daily mean cloud fraction < 20%) are considered, in order to
162 exclude interfering influences of clouds on the longwave radiation balance. Emissions from the lowest
163 atmospheric level correspond to DLR and emission from the uppermost level correspond to OLR. The
164 calculations are performed for eight different European sub-regions, adopted from the PRUDENCE
165 project (Christensen & Christensen, 2007), shown as red rectangles in Fig. 1.

166 The advantage of such an offline model is that numerous simulations can be performed, in which each
167 component affecting DLR and OLR, can be individually varied. In this way, the sensitivity of DLR and
168 OLR to changes in T_s , T_a and Q_a can be quantified. Subsequently, the respective proportion of each
169 component to changes in DLR and OLR can be quantified by means of a Taylor expansion, whereby the
170 derived sensitivities from the offline simulations constitute the partial derivatives of the Taylor
171 expansion (Shine & Sinha, 1991; Huang et al., 2007). Finally, the individual contributions of T_s , T_a and
172 Q_a to the simulated afforestation effects on DLR and OLR with CCLM-VEG3D are derived by multiplying
173 the changes in the temperature and humidity profiles with the partial derivatives of T_s , T_a and Q_a .

174



175 **3. Results**

176 **3.1. CCLM-VEG3 results**

177 **3.1.1 Effects on mean surface temperatures**

178 Fig. 2a shows the differences in DLR between CARBON and FOREST over the whole simulation period
179 (absolute values are shown in the supplement). Differences between both RCM simulations are only
180 caused by biogeochemical effects of afforestation. DLR is reduced in CARBON across Europe, as a result
181 of the reduced CO₂ concentrations. This reduced greenhouse effect leads to slightly reduced yearly
182 mean T_s in CARBON (Fig. 2b). However, the impact of this biogeochemical effect on T_s is negligible in
183 comparison to the biogeophysically induced changes of T_s (Fig. 2c and Fig. 2d). Fig. 2c shows the
184 differences between FOREST and GRASS for the yearly mean T_s in Europe. Differences between these
185 simulations are only caused by biogeophysical changes with afforestation. The magnitude of the
186 differences between FOREST and GRASS is much higher than between CARBON and FOREST, where
187 only biogeochemical effects are considered. The differences between CARBON and GRASS (Fig. 2d),
188 which can be considered as the total effect of afforestation, since both biogeochemical and
189 biogeophysical processes are taken into account, are consequently mainly caused by biogeophysical
190 processes and of the same magnitude as the differences between FOREST and GRASS. Thus, even with
191 an idealized reduction of the global CO₂ concentrations to pre-industrial levels by a Europe-wide
192 afforestation, the regional climate response to afforestation would be mainly dominated by
193 biogeophysical effects.

194

195 **3.1.2. Effects on the longwave radiation balance**

196 Fig. 3 shows the differences between the CARBON and the GRASS simulation for DLR (a+c) and OLR
197 (b+d) for the winter season (a+b) and the summer season (c+d). In winter, DLR is enhanced all over
198 Europe by afforestation, except of the Iberian Peninsula (IP). This extensive increase in DLR is
199 counterintuitive, since one would rather expect a reduction in DLR due to the reduced atmospheric
200 CO₂ concentrations with afforestation. OLR is also increased in winter all over Europe, which is in turn
201 in line with the reduced atmospheric CO₂ concentrations. In summer, a dipole in the DLR differences
202 between CARBON and GRASS is simulated, with a reduced DLR in central and southern Europe and an
203 increased one in Scandinavia (SC). A similar spatial pattern is simulated for OLR in summer with slightly
204 increased (reduced) OLR in northern Europe (southern Europe).

205

206 **3.2. BUGSrad results**

207 Fig. 4 shows the differences in DLR (a+c) and OLR (b+d) for the winter (a+b) and the summer season
208 (c+d) between CARBON and GRASS simulated with the BUGSrad radiative transfer model. The blue
209 bars show the total differences in DLR or OLR calculated by the offline model. The other colored bars



210 show the respective contributions of CO₂ (pink), Q_a (green), T_a (yellow) and T_s (black) to changes in DLR
211 and OLR between CARBON and GRASS. Thus, the black, yellow and green bars represent the
212 biophysical effects on the longwave radiation balance with afforestation, the pink bars the
213 biogeochemical ones. The grey bar is the residuum, which is attributed to non-linear effects.

214 The simulated differences between CARBON and GRASS with BUGSrad are in good agreement with the
215 results of CCLM-VEG3D. The calculated tendencies of afforestation are similar for the different regions
216 and seasons. BUGSrad is also simulating a Europe-wide increase in DLR (except of IP) and OLR in winter
217 in accordance with CCLM-VEG3D. The radiative dipole in summer with increased DLR and OLR in
218 northern Europe and reduced DLR and OLR in southern Europe is also consistently simulated with both
219 models. However, the absolute simulated differences between CARBON and GRASS can be different in
220 some regions or seasons. For instance, the reduction in OLR in SC in summer with afforestation is
221 stronger pronounced in BUGSrad than in CCLM-VEG3D, which is also the case for the reduction in DLR
222 in winter in IP. These differences are most likely caused by the different numbers of shortwave and
223 longwave bands in CCLM-VEG3D and BUGSrad.

224 The linearization of the differences in longwave radiation between CARBON and GRASS with BUGSrad
225 reveals that the increased DLR with afforestation in winter is primarily a result of biogeophysical
226 effects, compensating the attenuating effect of reduced CO₂ concentrations (negative pink bars) on
227 DLR (Fig. 4a). In this context, especially T_s has a strong impact on the differences in DLR (positive black
228 bars). Warmer T_s in winter (Fig. 5a), caused by the masking effect of snow on trees (Essery, 2013),
229 increase the longwave radiation emitted from the surface (except of IP where snow is not occurring
230 and T_s is reduced). As a result, more longwave radiation can be absorbed by the atmosphere and
231 reemitted as DLR to the surface. This positive feedback on the DLR is amplified by warmer T_a (increased
232 sensible heat fluxes, Fig. 6a) and an increased Q_a (increased evapotranspiration rates, Fig. 6b), which
233 have both a reinforcing effect on DLR (positive yellow and green bars). Thus, DLR is enhanced in winter
234 with afforestation although the CO₂ concentrations are reduced.

235 The same biogeochemical and biogeophysical changes of the longwave radiation balance lead to an
236 increase in OLR (Fig. 4b). The increased longwave radiation emissions, caused by the increased T_s,
237 provide more radiative energy that can be released into space (positive black bars). Simultaneously,
238 more longwave radiation can escape the atmosphere, due to reduced CO₂ concentrations (positive
239 pink bars). Therefore, biophysical and biochemical processes amplify each other, resulting in increased
240 OLR given afforestation all over Europe.

241 In contrast to the increased T_s in winter, T_s is reduced in summer with afforestation (Fig. 5b). The
242 longwave radiation emitted from the surface is consequently reduced and less radiative energy can be
243 absorbed and reemitted by the atmosphere (negative black bars in Fig. 4c). In combination with the
244 reduced CO₂ concentrations (negative pink bars), DLR is therefore reduced all over Europe, except of



245 SC (Fig. 4c). There, the T_s reduction with afforestation is quite small (Fig. 5b) and the reduction of
246 longwave radiation emitted from the surface is not as clear as for other areas (slightly negative black
247 bar), thus remaining on a comparatively high level. Additionally, evapotranspiration is strongly
248 increased in SC in summer (Fig. 6d), leading to increased Q_a in the lower troposphere (not shown).
249 Since water vapor is an effective greenhouse gas, increased concentrations contribute to an enhanced
250 absorption of the (just slightly reduced) longwave radiation emitted by the surface (clearly positive
251 green bar in SC). In this way, the biogeophysically induced changes of DLR compensate the attenuating
252 effect of reduced CO_2 concentrations on DLR in SC (negative pink bar).

253 Fig. 4d shows that biogeophysical and biogeochemical changes with afforestation have opposing
254 effects on OLR during summer. However, colder T_s reduce the longwave radiation emissions from the
255 surface, and thus the radiative energy that can be released into space (negative black bars). On the
256 other hand, reduced CO_2 concentrations in the atmosphere lead to a reduced absorption of longwave
257 radiation and more radiation that can pass the atmosphere (positive pink bars). Over central Europe
258 (ME), both processes balance each other leading to a net zero effect. In northern Europe (SC, BI),
259 biogeochemical effects are dominating, since changes in T_s and thus, the longwave radiation emissions
260 are especially in SC quite small. This process is stronger pronounced in BUGSrad than in CCLM-VEG3D.
261 Over southern and eastern Europe (MD, EA), the impact of the biogeophysical changes on OLR is
262 dominating. Here, the reduced longwave radiation emissions of the colder surface are amplified by
263 increased Q_a in the mid-troposphere (not shown), counteracting the effect of the reduced CO_2
264 concentrations.

265

266 3.3. TOA Energy Balance

267 The decomposition of the BUGSrad simulations showed that biogeophysical effects of afforestation
268 have a strong impact on the longwave radiation balance. The weakening of the greenhouse effect with
269 afforestation does consequently not only depend on the removal of CO_2 from the atmosphere. In
270 considering both biogeophysical and biogeochemical effects, the question arises, whether
271 afforestation has in general a warming or a cooling effect on the regional climate in Europe. In order
272 to investigate that, the energy balance at the top of the atmosphere (TOA) is analyzed. With this aim,
273 the net shortwave radiation input is compared to the net longwave radiation leaving the earth system.
274 In this way, biogeophysical changes in the shortwave radiation balance with afforestation by a reduced
275 surface albedo can be related to changes in the longwave radiation balance, which is affected by both
276 biogeophysical and biogeochemical process, as demonstrated above.

277 Changes in the TOA energy budget between CARBON and GRASS are shown for (a) winter, (b) summer
278 and (c) the whole year in Fig. 7. Red areas indicate regions in which afforestation leads to an increased
279 energy input into the regional climate system in Europe, blue areas indicate regions with a reduced



280 energy input. In winter, the TOA energy budget is positive in southern Europe, the Alpine region,
281 eastern Europe and southern Scandinavia (Fig. 7a). In these regions, the increased longwave radiative
282 energy loss by an increased OLR is compensated by an increased shortwave radiation input. In central
283 Europe, the British Isles and northern Scandinavia, the opposite is the case and the TOA energy budget
284 is negative or close to zero.

285 In summer, the interplay between changes in OLR and changes in the shortwave radiation lead to a
286 negative TOA energy budget in central and north-eastern Europe and a strongly positive energy budget
287 in southern Europe as well as parts of Scandinavia (Fig. 7b). Across seasons, the TOA energy budget is
288 almost all over Europe positive with afforestation (Fig. 7c), and the positive TOA energy budget in
289 Scandinavia is explained by a strong increase in the net shortwave radiation in spring (Fig. 8), due to
290 differences in the snow cover. Afforestation is consequently associated with a positive TOA energy
291 budget over Europe.

292

293 **4. Discussion**

294 Prior to the CARBON simulation, a global atmospheric CO₂ concentration of 279 ppm was calculated
295 as a response to a Europe-wide afforestation at the beginning of our simulation period (1986, see
296 section 2.2). At first glance, this substantial reduction of the global CO₂ concentration to pre-industrial
297 levels is astonishing. However, it has to be considered that the applied method is designed for a mature
298 forest, under the assumption of an equilibrium in the atmosphere-ocean system, which will be
299 achieved only on centennial timescales (Goodwin et al., 2007). An inertial short-term adjustment of
300 the CO₂ concentrations is therefore not considered. In addition, the presented study is an idealized
301 and simplified afforestation experiment, starting from a grassland continent. Thus, it is not a realistic
302 afforestation scenario (Bastin et al., 2019) and areas are afforested, in which the environmental
303 conditions are not actually ideal. Changes in the environmental conditions due to climate change are
304 also not considered. Moreover, ongoing fossil fuel emissions are neglected (Jones et al., 2016) and the
305 carbon already stored in grasslands (soil + biomass) is also not taken into account (Jackson et al., 2002).
306 The real carbon sequestration potential of afforestation should consequently be lower and the
307 reduction in global CO₂ concentrations, associated with a more realistic afforestation scenario, should
308 thus be smaller. Hence, this also means that the effect of biogeophysical processes on the longwave
309 radiation balance is likely to be even stronger in comparison to biogeochemical processes. Thus, the
310 regional warming effect of afforestation in Europe is expected to be even more intense in a realistic
311 setup. This experiment should thus be considered as sensitivity study by which the maximum potential
312 effect of afforestation on the longwave radiation balance and the regional climate was estimated.

313 Such a quantification of the direct impacts of biogeophysical and biogeochemical processes on changes
314 in the longwave radiation balance with afforestation is only possible within idealized RCM simulations,



315 since the indirect effects of global climate feedbacks can be specifically excluded. Moreover, the
316 advantage of RCM simulations is that the physical processes related to the interactions between the
317 land surface (soil and vegetation) and the atmosphere are better resolved than in global climate
318 simulations, whereby relevant land-atmosphere feedbacks are simulated more accurately on the
319 regional scale.

320 However, not all effects of afforestation on the European climate can be fully described on the basis
321 of the applied RCM approach. First, CO₂ dynamics are not considered in the CCLM-VEG3D simulations,
322 since no carbon cycle (Liski et al., 2005) is implemented in the modeling framework. Furthermore, all
323 simulations are driven by ERA-Interim reanalysis, which means present-day atmospheric conditions
324 with recent CO₂ concentrations. The feedbacks of reduced CO₂ concentrations and biogeophysical
325 effects on the global climate system, especially on ocean-atmosphere interactions (Davin & de Noblet-
326 Ducoudré 2010; Swann et al., 2012) as well as on snow and sea ice cover (Donohoe et al., 2014), are
327 consequently not considered.

328 These missing global feedbacks are most likely the reason for the small effects on simulated T_s in
329 Europe by an atmospheric CO₂ reduction to pre-industrial levels (Fig. 2b). This small temperature effect
330 is apparently in contradiction to observations, documenting that increasing CO₂ concentrations led to
331 a considerable warming of up to 1.5 K in Europe until the end of our simulation period in comparison
332 to pre-industrial levels (EEA, 2017). However, the results of our simulations are in line with recent
333 studies providing evidence that the temperature effect of changing CO₂ concentrations is not directly
334 caused by changes in the longwave radiation balance, but indirectly induced by changes in global
335 climate feedbacks, like changes in the snow and sea ice cover (e.g., Donohoe et al., 2014). Since such
336 feedbacks are not included in our experiment, we have to conclude that the driving boundary
337 conditions of our simulations are too warm.

338 Against this background, we can assume that an idealized reduction of the global CO₂ concentrations
339 to pre-industrial conditions by a regional afforestation would have a global cooling effect, due to the
340 global climate feedbacks described above. A consideration of such colder global climate conditions in
341 our experiment would of course have certain implications on the biogeophysical processes in our
342 modeling domain. For instance, driving the CARBON simulation with generally colder boundary
343 conditions would enhance snowfall during winter in Europe. The snow masking effect would
344 consequently be increased and more solar radiation would be absorbed than with present-day
345 boundary conditions. As a result, the TOA energy budget would become more positive in winter. This
346 process is already known to be the reason for the general warming effect of afforestation in the high
347 latitudes (e.g. Claussen et al., 2001; Bonan, 2008). Furthermore, more snow accumulation in winter
348 would extent the melting phase in spring and increase the differences in absorbed solar radiation
349 between CARBON and GRASS. Since an increased net shortwave radiation in spring (Fig. 8) is already



350 an important factor for the positive TOA energy budget with afforestation particularly in Scandinavia,
351 the total warming would be increased.

352 In addition, the impact of wind shear on the turbulent heat exchange is getting stronger for colder
353 atmospheric conditions, since buoyance is getting smaller (e.g. Breil et al., 2021). That means that the
354 impact of the surface roughness on T_s is also getting stronger. Since the surface roughness of forests is
355 higher than of grasslands, the summertime cooling effect of afforestation on T_s (Fig. 5b) would be
356 increased and emitted longwave radiation would be further reduced. Therefore, the consideration of
357 global climate feedbacks in our modeling approach and thus, a forcing with colder boundary
358 conditions, would even intensify the positive TOA energy budget and the warming effect of
359 afforestation in Europe. An idealized reduction of the global CO_2 concentrations to pre-industrial levels
360 by afforestation would consequently not actually cool the regional climate in Europe to pre-industrial
361 conditions, as the regionally increased TOA energy budget would counteract the global effect.

362

363 5. Conclusions

364 In this study, the general effects of biogeophysical and biogeochemical processes on the longwave
365 radiation balance and the regional climate conditions in Europe are analyzed within an idealized
366 Europe-wide afforestation RCM experiment, in which the global CO_2 concentrations were reduced to
367 pre-industrial levels at the beginning of our simulation period. The respective contributions of
368 biogeophysical and biogeochemical effects were decomposed by means of additional offline
369 simulations with a radiative transfer model.

370 Results show that the impact of biogeochemical processes with afforestation on surface temperature
371 (T_s) is negligible in comparison to the biogeophysical effects (Fig. 2). Beyond that, biogeophysical
372 processes affect the regional longwave radiation balance, which is generally thought to be positively
373 influenced by afforestation, due to the net removal of CO_2 from the atmosphere. However, our results
374 provide evidence that biogeophysically induced changes of T_s , T_a and Q_a are at least as important for
375 the longwave radiation balance as the atmospheric CO_2 reduction (Fig. 3 and 4). In particular, the
376 changes in T_s have a considerable impact on the magnitude of the greenhouse effect, in line with
377 Vargas Zeppetello et al. (2019).

378 While results based on coarser resolved global climate studies rather indicate so far that
379 biogeophysical and biogeochemical effects balance each other in Europe (Claussen et al., 2001, Bala
380 et al., 2007), we provide here clear evidence that afforestation as implemented in our simulations has
381 a total warming effect on the regional climate (Fig. 7). Thus, the increased shortwave radiation input
382 due to the biogeophysical reduction of the surface albedo, is not compensated by increased longwave
383 radiation emissions, associated with reduced CO_2 concentrations. Even with an idealized reduction of
384 the global CO_2 concentrations to pre-industrial levels, the European climate response would still be



385 dominated by biogeophysical processes associated with Europe-wide afforestation. A sole
386 consideration of forests carbon sequestration potential is therefore not enough to assess the suitability
387 of afforestation as mitigation strategy. We conclude that biogeophysical effects always need to be
388 taken into account comprehensively, particularly as they affect the regional greenhouse effect, which
389 is the reason for the generally positive assessment of afforestation as mitigation strategy.

390

391 **Code availability**

392 The code of CCLM-VEG3D is available upon request from the corresponding author. The code of
393 BUGSrad is available on the BUGSrad GitHub repository (<https://github.com/mattchri/BUGSrad>, last
394 access: 16 November 2022).

395

396 **Data availability**

397 The data that support the findings of this study are available upon reasonable request from the
398 corresponding author.

399

400 **Author contribution**

401 MB designed the study and wrote the paper. MB and FK performed the CCLM-VEG3D simulations and
402 FK performed the BUGSrad simulations. FK analyzed the data and prepared the figures. All authors
403 contributed with discussion, interpretation of results and text revisions.

404

405 **Competing interests**

406 The authors declare that they have no conflict of interest.

407

408 **Financial Support**

409 JGP thanks the AXA Research Fund for support.

410

411 **Acknowledgements**

412 All authors thank Peter Knippertz for the fruitful discussions and his scientific input.

413

414

415

416

417

418

419



420 **References**

421 Alkama, R., and Cescatti, A.: Biophysical climate impacts of recent changes in global forest cover.
422 *Science*, 351(6273), 600-604. DOI: [10.1126/science.aac8083](https://doi.org/10.1126/science.aac8083), 2016.

423

424 Bala, G., Caldeira, K., Wickett, M., Phillips, T. J., Lobell, D. B., Delire, C., and Mirin, A.: Combined climate
425 and carbon-cycle effects of large-scale deforestation. *Proceedings of the National Academy of Sciences*,
426 104(16), 6550-6555. <https://doi.org/10.1073/pnas.0608998104>, 2007.

427

428 Bastin, J. F., Finegold, Y., Garcia, C., Mollicone, D., Rezende, M., Routh, D., Zohner, C., and Crowther, T.
429 W.: The global tree restoration potential. *Science*, 365(6448), 76-79. DOI: [10.1126/science.aax0848](https://doi.org/10.1126/science.aax0848),
430 2019.

431

432 Bonan, G. B.: Forests and climate change: forcings, feedbacks, and the climate benefits of forests.
433 *Science*, 320(5882), 1444-1449. DOI: [10.1126/science.1155121](https://doi.org/10.1126/science.1155121), 2008.

434

435 Burakowski, E., Tawfik, A., Ouimette, A., Lepine, L., Novick, K., Ollinger, S., Zarzycki, C., and Bonan, G.:
436 The role of surface roughness, albedo, and Bowen ratio on ecosystem energy balance in the Eastern
437 United States. *Agricultural and Forest Meteorology*, 249, 367-376.
438 <https://doi.org/10.1016/j.agrformet.2017.11.030>, 2018.

439

440 Breil, M., Davin, E. L., and Rechid, D.: What determines the sign of the evapotranspiration response to
441 afforestation in European summer? *Biogeosciences*, 18(4), 1499-1510. [https://doi.org/10.5194/bg-18-
442 1499-2021](https://doi.org/10.5194/bg-18-1499-2021), 2021.

443

444 Breil, M., Rechid, D., Davin, E. L., de Noblet-Ducoudré, N., Katragkou, E., Cardoso, R. M., Hoffmann, P.,
445 Jach, L.L., Soares, P.M.M., Sofiadis, G., Strada, S., Strandberg, G., Tölle, M.H., and Warrach-Sagi, K.: The
446 opposing effects of reforestation and afforestation on the diurnal temperature cycle at the surface and
447 in the lowest atmospheric model level in the European summer. *Journal of Climate*, 33(21), 9159-9179.
448 <https://doi.org/10.1175/JCLI-D-19-0624.1>, 2020.

449

450 Bright, R. M., Davin, E., O'Halloran, T., Pongratz, J., Zhao, K., and Cescatti, A.: Local temperature
451 response to land cover and management change driven by non-radiative processes. *Nature Climate
452 Change*, 7(4), 296-302. <https://doi.org/10.1038/nclimate3250>, 2017.

453



- 454 Christensen, J. H., and Christensen, O. B.: A summary of the PRUDENCE model projections of changes
455 in European climate by the end of this century. *Climatic change*, 81(1), 7-30.
456 <https://doi.org/10.1007/s10584-006-9210-7>, 2007.
- 457
- 458 Claussen, M., Brovkin, V., and Ganopolski, A.: Biogeophysical versus biogeochemical feedbacks of
459 large-scale land cover change. *Geophysical research letters*, 28(6), 1011-1014.
460 <https://doi.org/10.1029/2000GL012471>, 2001.
- 461
- 462 Davin, E. L., and de Noblet-Ducoudré, N.: Climatic impact of global-scale deforestation: Radiative
463 versus nonradiative processes. *Journal of Climate*, 23(1), 97-112.
464 <https://doi.org/10.1175/2009JCLI3102.1>, 2010.
- 465
- 466 Davin, E. L., Rechid, D., Breil, M., Cardoso, R. M., Coppola, E., Hoffmann, P., Jach, L. L., Katragkou, E.,
467 de Noblet-Ducoudré, N., Radtke, K., Raffa, M., Soares, P. M. M., Sofiadis, G., Strada, S., Strandberg, G.,
468 Tölle, M. H., Warrach-Sagi, K., and Wulfmeyer, V.: Biogeophysical impacts of forestation in Europe: first
469 results from the LUCAS (Land Use and Climate Across Scales) regional climate model intercomparison.
470 *Earth System Dynamics*, 11(1), 183-200. <https://doi.org/10.5194/esd-11-183-2020>, 2020.
- 471
- 472 Dee, D. P., Uppala, S. M., Simmons, A. J., Berrisford, P., Poli, P., Kobayashi, S., Andrae, U., Balmaseda,
473 M. A., Balsamo, G., Bauer, P., Bechthold, P., Beljaars, A. C. M., van de Berg, L., Bidlot, J., Bormann, N.,
474 Delsol, C., Dragani, R., Fuentes, M., Geer, A. J., Haimberger, L., Healy, S. B., Hersbach, H., Holm, E. V.,
475 Isaksen, L., Kallberg, P., Köhler, M., Matricardi, M., McNally, A. P., Monge-Sanz, B. M., Morcrette, J.-J.,
476 Park, B.-K., Peubey, C., de Rosnay, P., Tavolato, C., Thepaut, J.-N., and Vitart, F.: The ERA-Interim
477 reanalysis: Configuration and performance of the data assimilation system. *Quarterly Journal of the*
478 *royal meteorological society*, 137(656), 553-597. <https://doi.org/10.1002/qj.828>, 2011.
- 479
- 480 Donohoe, A., Armour, K. C., Pendergrass, A. G., and Battisti, D. S.: Shortwave and longwave radiative
481 contributions to global warming under increasing CO₂. *Proceedings of the National Academy of*
482 *Sciences*, 111(47), 16700-16705, 2014.
- 483
- 484 Duveiller, G., Hooker, J., and Cescatti, A.: The mark of vegetation change on Earth's surface energy
485 balance. *Nature communications*, 9(1), 1-12. <https://doi.org/10.1038/s41467-017-02810-8>, 2018.
- 486
- 487 EEA, C. C.: Impacts and vulnerability in europe 2016—an indicator-based report. Luxembourg:
488 Publications Office of the European Union, 1, 2017.



489
490 Essery, R.: Large-scale simulations of snow albedo masking by forests. *Geophysical Research Letters*,
491 *40*(20), 5521-5525. <https://doi.org/10.1002/grl.51008>, 2013.
492
493 Friedlingstein, P., O'Sullivan, M., Jones, M. W., Andrew, R. M., Hauck, J., Olsen, A., Peters, G. P., Peters,
494 W., Pongratz, J., Sitch, S., Le Quéré, C., Canadell, J. G., Ciais, P., Jackson, R. B., Alin, S., Aragão, L. E. O.
495 C., Arneeth, A., Arora, V., Bates, N. R., Becker, M., Benoit-Cattin, A., Bittig, H. C., Bopp, L., Bultan, S.,
496 Chandra, N., Chevallier, F., Chini, L. P., Evans, W., Florentie, L., Forster, P. M., Gasser, T., Gehlen, M.,
497 Gilfillan, D., Gkritzalis, T., Gregor, L., Gruber, N., Harris, I., Hartung, K., Haverd, V., Houghton, R. A.,
498 Ilyina, T., Jain, A. K., Joetzjer, E., Kadono, K., Kato, E., Kitidis, V., Korsbakken, J. I., Landschützer, P.,
499 Lefèvre, N., Lenton, A., Lienert, S., Liu, Z., Lombardozzi, D., Marland, G., Metzl, N., Munro, D. R., Nabel,
500 J. E. M. S., Nakaoka, S.-I., Niwa, Y., O'Brien, K., Ono, T., Palmer, P. I., Pierrot, D., Poulter, B., Resplandy,
501 L., Robertson, E., Rödenbeck, C., Schwinger, J., Séférian, R., Skjelvan, I., Smith, A. J. P., Sutton, A. J.,
502 Tanhua, T., Tans, P. P., Tian, H., Tilbrook, B., van der Werf, G., Vuichard, N., Walker, A. P., Wanninkhof,
503 R., Watson, A. J., Willis, D., Wiltshire, A. J., Yuan, W., Yue, X., and Zaehle, S.: Global Carbon Budget
504 2020, *Earth Syst. Sci. Data*, *12*, 3269–3340, <https://doi.org/10.5194/essd-12-3269-2020>, 2020.
505
506 Goodwin, P., Williams, R. G., Follows, M. J., and Dutkiewicz, S.: Ocean-atmosphere partitioning of
507 anthropogenic carbon dioxide on centennial timescales. *Global Biogeochemical Cycles*, *21*(1), GB1014,
508 <https://doi.org/10.1029/2006GB002810>, 2007.
509
510 Gütschow, J., Jeffery, L., Gieseke, R., and Günther, A.: The PRIMAP-hist national historical emissions
511 time series (1850-2017). V. 2.1. GFZ Data Services. <https://doi.org/10.5880/PIK.2019.018>, 2019.
512
513 Harper, A. B., Powell, T., Cox, P. M., House, J., Huntingford, C., Lenton, T. M., Sitch, S., Burke, E.,
514 Chadburn, S. E., Collins, W. J., Comyn-Platt, E., Daioglou, V., Doelman, J. C., Hayman, G., Robertson, E.,
515 van Vuuren, D., Wiltshire, A., Webber, C. P., Bastos, A., Boysen, L., Ciais, P., Devaraju, N., Jain, A. K.,
516 Krause, A., Poulter, B., and Shu, S.: Land-use emissions play a critical role in land-based mitigation for
517 Paris climate targets. *Nature communications*, *9*(1), 1-13. [https://doi.org/10.1038/s41467-018-05340-](https://doi.org/10.1038/s41467-018-05340-z)
518 [z](https://doi.org/10.1038/s41467-018-05340-z), 2018.
519
520 Huang, Y., Ramaswamy, V., and Soden, B.: An investigation of the sensitivity of the clear-sky outgoing
521 longwave radiation to atmospheric temperature and water vapor. *Journal of Geophysical Research:*
522 *Atmospheres*, *112*, D05104. <https://doi.org/10.1029/2005JD006906>, 2007.
523



- 524 Jackson, R. B., Banner, J. L., Jobbágy, E. G., Pockman, W. T., and Wall, D. H.: Ecosystem carbon loss with
525 woody plant invasion of grasslands. *Nature*, 418(6898), 623-626.
526 <https://doi.org/10.1038/nature00910>, 2002.
- 527
- 528 Jacob, D., Petersen, J., Eggert, B., Alias, A., Christensen, O. B., Bouwer, L. M., Braun, A., Colette, A.,
529 Deque, M., Georgievski, G., Georgopoulou, E., Gobiet, A., Menut, L., Nikulin, G., Haensler, A.,
530 Hempelmann, N., Jones, C., Keuler, K., Kovats, S., Kröner, N., Kotlarski, S., Kriegsman, A., Martin, E.,
531 van Meijgaard, E., Moseley, C., Pfeifer, S., Preuschmann, S., Radermacher, C., Radtke, K., Rechid, D.,
532 Rounsevell, M., Samuelsson, P., Somot, S., Soussana J.-F., Teichmann, C., Valentini, R., Vautard, R.,
533 Weber, B., and Yiou, P.: EURO-CORDEX: new high-resolution climate change projections for European
534 impact research. *Regional environmental change*, 14(2), 563-578. [https://doi.org/10.1007/s10113-](https://doi.org/10.1007/s10113-013-0499-2)
535 [013-0499-2](https://doi.org/10.1007/s10113-013-0499-2), 2014.
- 536
- 537 Jones, C. D., Ciais, P., Davis, S. J., Friedlingstein, P., Gasser, T., Peters, G. P., Rogelj, J., van Vuuren, D. P.,
538 Canadell, J. G., Cowie, A., Jackson, R. B., Jonas, M., Kriegler, E., Littleton, E., Lowe, J. A., Milne, J.,
539 Shrestha, G., Smith, P., Torvanger, A., and Wiltshire, A.: Simulating the Earth system response to
540 negative emissions. *Environmental Research Letters*, 11(9), 095012. [doi:10.1088/1748-](https://doi.org/10.1088/1748-9326/11/9/095012)
541 [9326/11/9/095012](https://doi.org/10.1088/1748-9326/11/9/095012), 2016.
- 542
- 543 Lawrence, P. J., and Chase, T. N.: Representing a new MODIS consistent land surface in the Community
544 Land Model (CLM 3.0). *Journal of Geophysical Research: Biogeosciences*, 112, G01023.
545 <https://doi.org/10.1029/2006JG000168>, 2007.
- 546
- 547 Lee, X., Goulden, M. L., Hollinger, D. Y., Barr, A., Black, T. A., Bohrer, G., Bracho, R., Drake, B., Goldstein,
548 A., Gu, L., Katul, G., Kolb, T., Law, B. E., Margolis, H., Meyers, T., Monson, R., Munger, W., Oren, R., Tha
549 Paw U, K., Richardson, A. D., Schmid, H.-P., Staebler, R., Wofsy, S., and Zhao, L.: Observed increase in
550 local cooling effect of deforestation at higher latitudes. *Nature*, 479(7373), 384-387.
551 <https://doi.org/10.1038/nature10588>, 2011.
- 552
- 553 Liski, J., Palosuo, T., Peltoniemi, M., and Sievänen, R.: Carbon and decomposition model Yasso for
554 forest soils. *Ecological modelling*, 189(1-2), 168-182.
555 <https://doi.org/10.1016/j.ecolmodel.2005.03.005>, 2005.
- 556
- 557 Luysaert, S., Ciais, P., Piao, S. L., Schulze, E. D., Jung, M., Zaehle, S., Schelhaas, M. J., Reichstein, M.,
558 Churkina, G., Papale, D., Abril, G., Beer, C., Grace, J., Loustau, D., Matteucci, G., Magnani, F., Nabuurs,



- 559 G. J., Verbeeck, H., Sulkava, M., van der Werf, G. R., Janssens, I. A., and members of the CARBOEUROPE-
560 IP SYNTHESIS TEAM: The European carbon balance. Part 3: forests. *Global Change Biology*, 16(5), 1429-
561 1450. <https://doi.org/10.1111/j.1365-2486.2009.02056.x>, 2010.
- 562
- 563 Pan, Y., Birdsey, R. A., Fang, J., Houghton, R., Kauppi, P. E., Kurz, W. A., .Phillips, O. L., Shvidenko, A.,
564 Lewis, S. L., Canadell, J. G., Ciais, P., Jackson, R. B., Pacala, S. W., McGuire, A. D., Paio, S., Rautiainen,
565 A., Sitch, S., and Hayes, D.: A large and persistent carbon sink in the world's forests. *Science*, 333(6045),
566 988-993. DOI: [10.1126/science.1201609](https://doi.org/10.1126/science.1201609), 2011.
- 567
- 568 Pielke Sr, R. A., Pitman, A., Niyogi, D., Mahmood, R., McAlpine, C., Hossain, F., Goldewijk, K. K., Nair,
569 U., Betts, R., Fall, S., Reichstein, M., Kabat, P., and de Noblet, N.: Land use/land cover changes and
570 climate: modeling analysis and observational evidence. *Wiley Interdisciplinary Reviews: Climate*
571 *Change*, 2(6), 828-850. doi: [10.1002/wcc.144](https://doi.org/10.1002/wcc.144), 2011.
- 572
- 573 Ritter, B., and Geleyn, J. F.: A comprehensive radiation scheme for numerical weather prediction
574 models with potential applications in climate simulations. *Monthly weather review*, 120(2), 303-325.
575 [https://doi.org/10.1175/1520-0493\(1992\)120<0303:ACRSFN>2.0.CO;2](https://doi.org/10.1175/1520-0493(1992)120<0303:ACRSFN>2.0.CO;2), 1992.
- 576
- 577 Roe, S., Streck, C., Obersteiner, M., Frank, S., Griscom, B., Drouet, L., Fricko, O., Gusti, M., Harris, N.,
578 Hasegawa, T., Hausfather, Z., Havlik, P., House, J., Nabuurs, G.-J., Popp, A., Sanz Sanchez, M. J.,
579 Sanderman, J., Smit, P., Stehfest, E., and Lawrence, D.: Contribution of the land sector to a 1.5 C world.
580 *Nature Climate Change*, 9(11), 817-828. <https://doi.org/10.1038/s41558-019-0591-9>, 2019.
- 581
- 582 Shine, K. P., and Sinha, A.: Sensitivity of the Earth's climate to height-dependent changes in the water
583 vapour mixing ratio. *Nature*, 354(6352), 382-384. <https://doi.org/10.1038/354382a0>, 1991.
- 584
- 585 Stephens, G. L., Gabriel, P. M., and Partain, P. T.: Parameterization of atmospheric radiative transfer.
586 Part I: Validity of simple models. *Journal of the atmospheric sciences*, 58(22), 3391-3409.
587 [https://doi.org/10.1175/1520-0469\(2001\)058<3391:POARTP>2.0.CO;2](https://doi.org/10.1175/1520-0469(2001)058<3391:POARTP>2.0.CO;2), 2001.
- 588
- 589 Swann, A. L., Fung, I. Y., Levis, S., Bonan, G. B., and Doney, S. C.: Changes in Arctic vegetation amplify
590 high-latitude warming through the greenhouse effect. *Proceedings of the National Academy of*
591 *Sciences*, 107(4), 1295-1300. <https://doi.org/10.1073/pnas.0913846107>, 2010.
- 592



593 Swann, A. L., Fung, I. Y., and Chiang, J. C.: Mid-latitude afforestation shifts general circulation and
594 tropical precipitation. *Proceedings of the National Academy of Sciences*, 109(3), 712-716.
595 <https://doi.org/10.1073/pnas.1116706108>, 2012.

596

597 Vargas Zeppetello, L. R., Donohoe, A., and Battisti, D. S.: Does surface temperature respond to or
598 determine downwelling longwave radiation? *Geophysical Research Letters*, 46(5), 2781-2789.
599 <https://doi.org/10.1029/2019GL082220>, 2019.

600

601

602

603

604

605

606

607

608

609

610

611

612

613

614

615

616

617

618

619

620

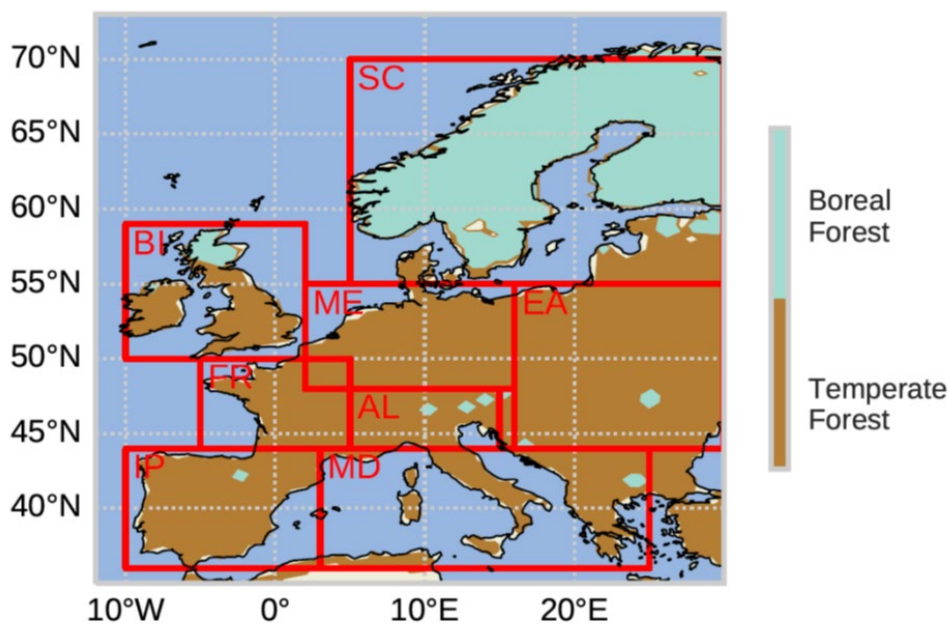
621

622

623

624

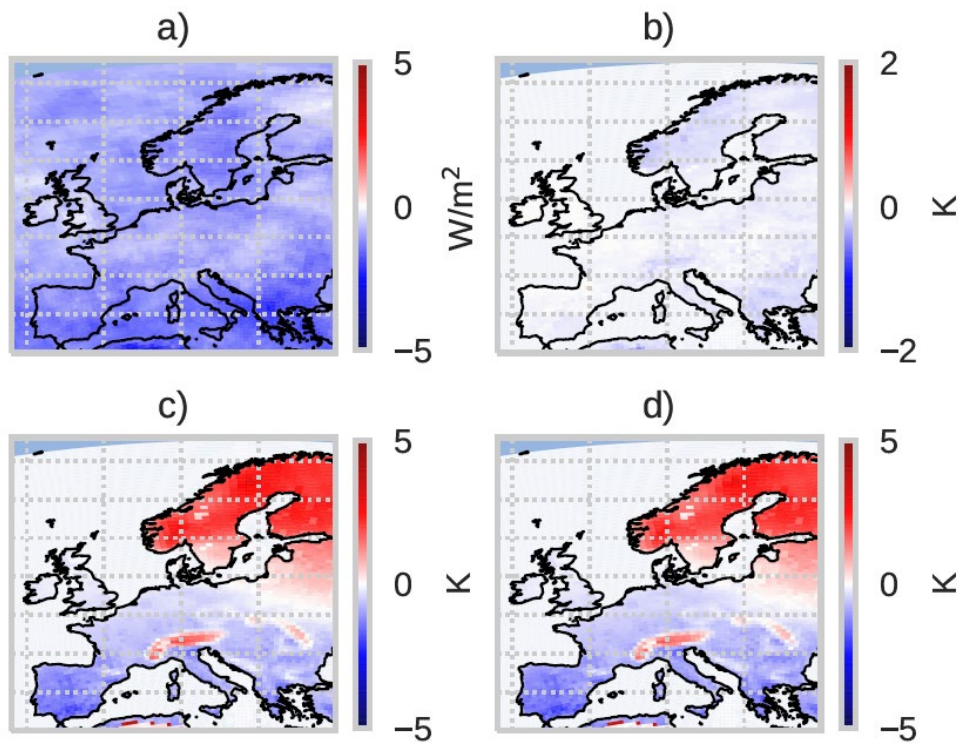
625



626

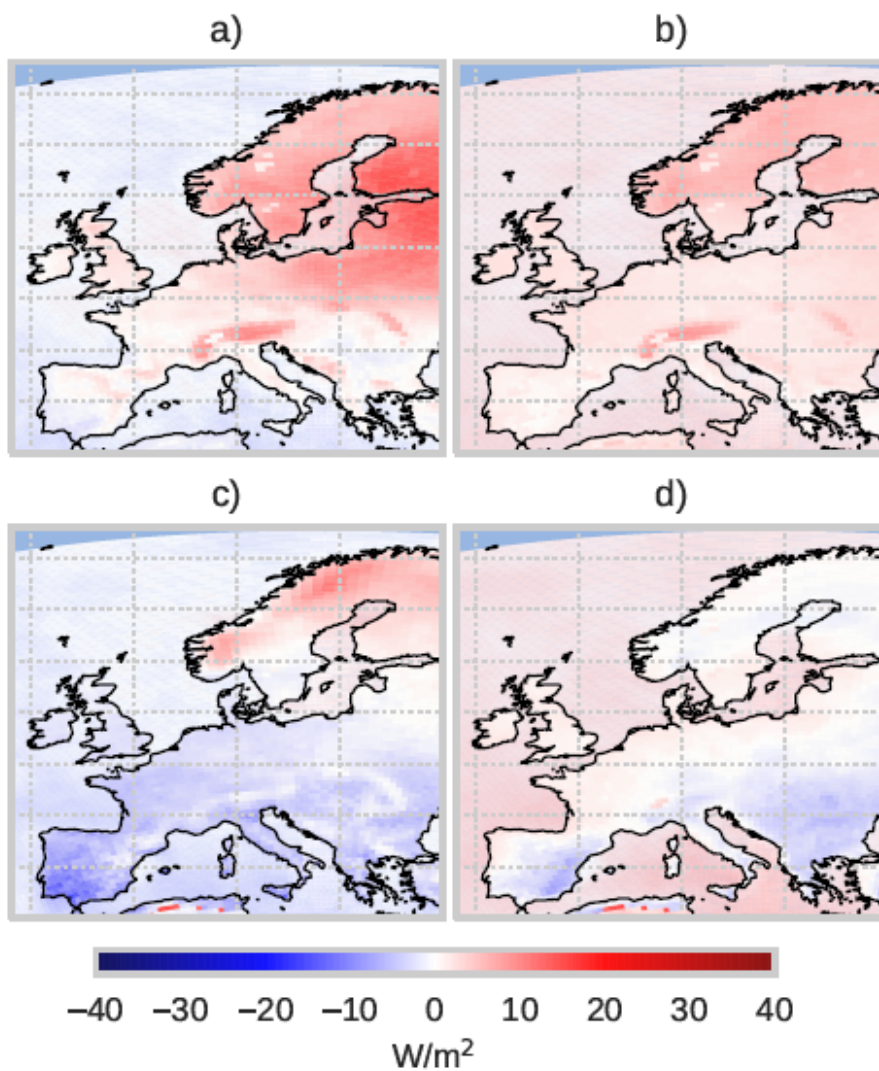
627 Figure 1: Spatial distribution of boreal and temperate forests in the CCLM-VEG3D FOREST and CARBON

628 simulations.



629
630 Figure 2: Yearly mean differences in (a) DLR and (b,c,d) T_s between (a+b) CARBON and FOREST, (c)
631 FOREST and GRASS, and (d) CARBON and GRASS for the period 1986-2015.

632
633
634
635
636
637
638
639
640
641
642
643
644
645



646

647 Figure 3: Differences between CARBON and GRASS for DLR (a+c) and OLR (b+d) for the winter season

648 (a+b) and the summer season (c+d) over the period 1986-2015.

649

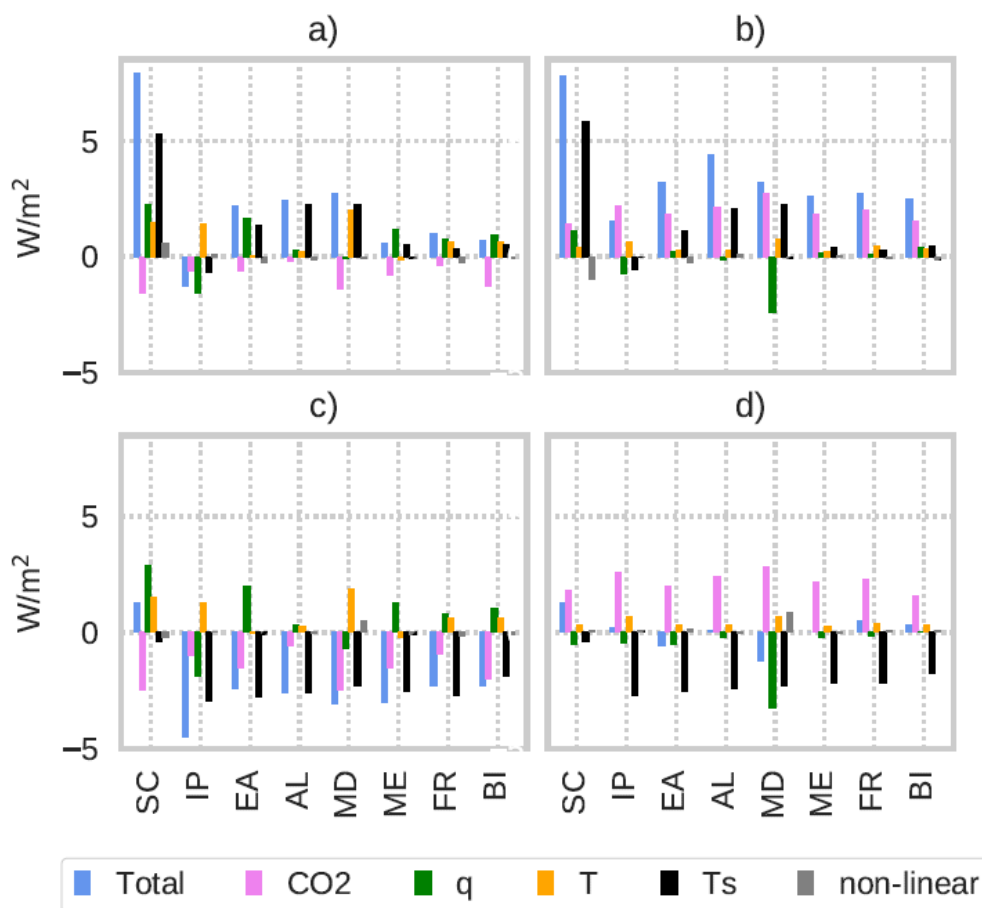
650

651

652

653

654



655

656 Figure 4: Differences in DLR (a+c) and OLR (b+d) for the winter (a+b) and the summer season (c+d)

657 between CARBON and GRASS simulated with BUGSrad. Blue bars show total differences in DLR/OLR.

658 The other bars show the respective contributions of CO₂ (pink), Q_a (green), T_a (yellow) and T_s (black) to

659 changes in DLR/OLR. Black, yellow and green bars represent biogeophysical effects on the longwave

660 radiation balance with afforestation, pink bars biogeochemical effects. The grey bar is the residuum,

661 which is attributed to non-linear effects.

662

663

664

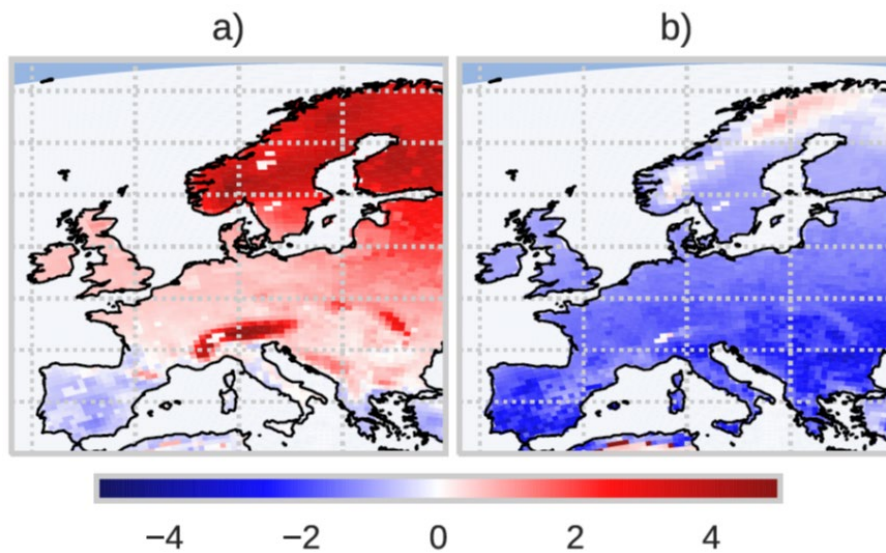
665

666

667

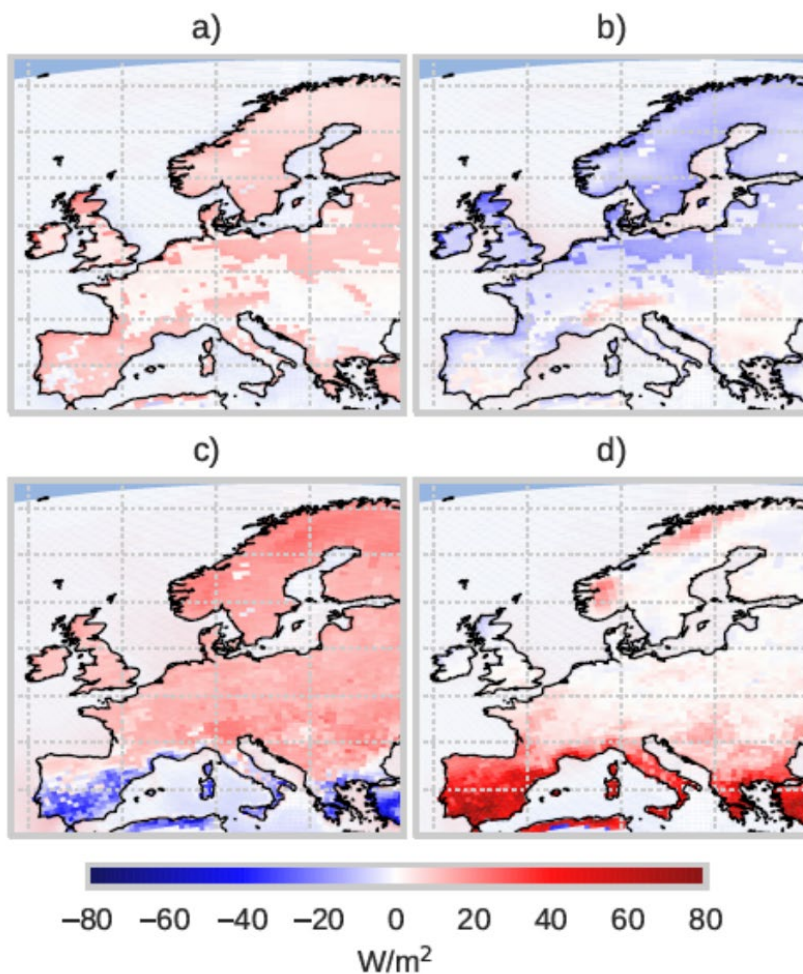
668

669

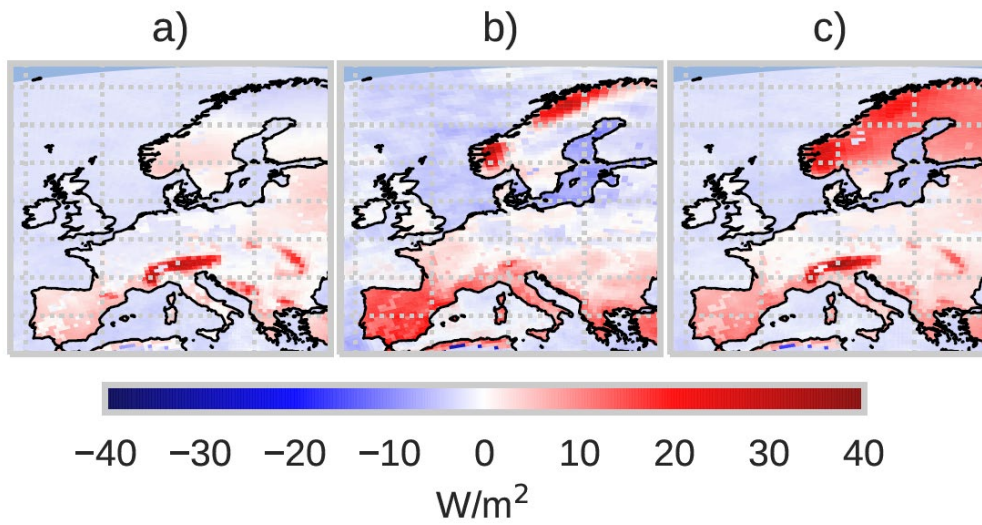


670
671 Figure 5: Mean differences in T_s in [K] between CARBON and GRASS for the period 1986-2015, for the
672 (a) winter season and the (b) summer season.

673
674
675
676
677
678
679
680
681
682
683
684
685
686
687
688
689
690
691



692
693 Figure 6: Mean differences between CARBON and GRASS for the period 1986-2015 in (a, b) winter
694 and (c, d) summer for the (a, c) sensible and (b, d) latent heat fluxes.
695



696

697 Figure 7: Changes in the TOA energy balance between CARBON and GRASS for (a) winter, (b) summer
698 and (c) the whole year.

699

700

701

702

703

704

705

706

707

708

709

710

711

712

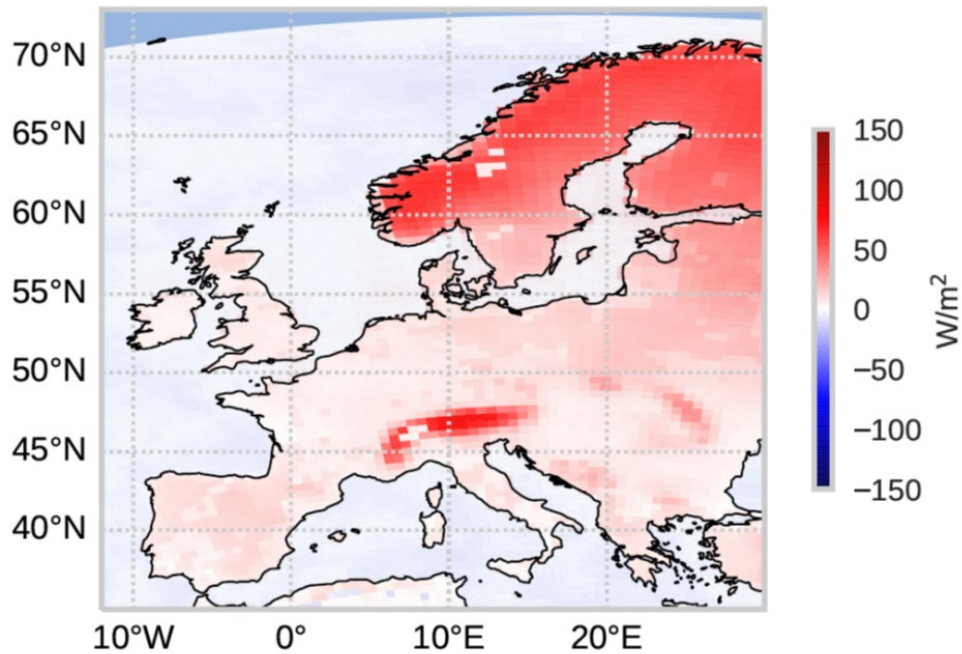
713

714

715

716

717



718

719 Figure 8: Mean differences in net shortwave radiation in spring between CARBON and GRASS for the
720 period 1986-2015.

721